1521-009X/47/2/164–172$35.00
DRUG METABOLISM AND DISPOSITION

https://doi.org/10.1124/dmd.118.083188
Drug Metab Dispos 47:164–172, February 2019



# Overcoming P-Glycoprotein–Mediated Drug Resistance with Noscapine Derivatives[S]

Divya Muthiah, Georgia K. Henshaw, Aaron J. DeBono, Ben Capuano, Peter J. Scammells, and Richard Callaghan

*Division of Biomedical Science and Biochemistry, Research School of Biology and Medical School, Australian National University, Canberra, Australian Capital Territory (D.M., G.K.H., R.C.), and Medicinal Chemistry, Monash Institute of Pharmaceutical Sciences, Monash University, Parkville, Victoria (A.J.D., B.C., P.J.S.), Australia*

Received June 20, 2018; accepted November 20, 2018

## ABSTRACT

**The antitussive agent noscapine has been shown to inhibit the proliferation of cancer cells by disruption of tubulin dynamic. However, the efficacy of several anticancer drugs that inhibit tublin dynamics (vinca alkaloids and taxanes) is reduced by the multidrug resistance phenotype. These compounds are substrates for P-glycoprotein (P-gp)–mediated extrusion from cells. Consequently, the antiproliferative activity of noscapine and a series of derivatives was measured in drug-sensitive and drug-resistant cells that overexpress P-gp. None of the noscapine derivatives displayed lower potency in cells overexpressing P-gp, thereby suggesting a lack of interaction with this pump. However, the cellular efflux of a fluorescent substrate by P-gp was potently inhibited by noscapine and most derivatives. Further investigation with purified, reconstituted P-gp demonstrated that inhibition of P-gp function was due to direct interaction of noscapine derivatives with the transporter. Moreover, coadministration of vinblastine with two of the noscapine derivatives displayed synergistic inhibition of proliferation, even in P-gp–expressing resistant cell lines. Therefore, noscapine derivatives offer a dual benefit of overcoming the significant impact of P-gp in conferring multidrug resistance and synergy with tubulin-disrupting anticancer drugs.**

## Introduction

The alkaloid noscapine is found in the opium poppy (*Papaver somniferum*) and belongs to the chemical class of phthalideisoquinolines. Noscapine is classified as an opiate, alongside morphine, thebaine, codeine, and papaverine. However, noscapine does not produce respiratory depression, sedation, or analgesia, and its main therapeutic use is as an antitussive agent (Empey et al., 1979; Dahlstrom et al., 1982; Mahmoudian and Rahimi-Moghaddam, 2009). Noscapine has a low-toxicity profile and is sufficiently water-soluble to be administered orally.

Based on the chemical similarity of noscapine to colchicine and the podophyllotoxins, the possibility of an interaction with tubulin was investigated (Ye et al., 1998). Noscapine was demonstrated to bind to tubulin, alter tubulin dynamics, and arrest mitosis at the $G_2$/M phase was investigated (Ye et al., 1998; Mahmoudian and Rahimi-Moghaddam, 2009), properties that are common to several anticancer agents, including vinca alkaloids and taxanes. The anticancer activity of noscapine was confirmed by its ability to inhibit the proliferation of cancer cells and the growth of solid tumors in vivo (Ye et al., 1998). Despite the comparatively low-toxicity profile of noscapine, its anticancer activity lacked potency, with growth inhibitory effects on cultured cells in the micromolar range. As a result, medicinal chemistry programs have generated several derivatives with the aim of generating greater potency.

A series of analogs was generated with halo substitutions at the 9′-position of noscapine (Fig. 1) with the goal of improving the potency of cell-cycle arrest (Aneja et al., 2006b). The 7′-position of noscapine was also targeted with the synthesis of carbamate or urea analogs (Anderson et al., 2005a,b) and a series of more bulky substitutions (Mishra et al., 2011). The N-demethylation of noscapine to yield nornoscapine provided a template for the introduction of multiple substitutions at the 6′-position (DeBono et al., 2012). Finally, a more recent investigation generated noscapine derivatives with multiple substitutions at the 6′, 7′, and 9′ positions (Debono et al., 2014). The series of compounds was divided into lactones (**2–5**) and cyclic ethers (**6–11**), with carbamate and urea derivatives and halogen substitutions. These combined medicinal chemistry efforts provided considerable information about the structure-activity relationship for noscapine. The new derivatives displayed improved affinity of interaction with tubulin, greater potency to inhibit cell proliferation, and increased cell-cycle arrest at the $G_2$/M phase.

The ability of noscapine to interfere with tubulin dynamics raises the possibility of synergism with anticancer drugs that also target tubulin dynamics, for example, vinblastine and paclitaxel. It is noteworthy, however, that the efficacy of both these drugs is markedly reduced by the resistance modifier P-glycoprotein (P-gp) (Dumontet et al., 1996; Martin et al., 1999). P-gp is a member of the ATP-binding cassette (ABC) superfamily of transport proteins and mediates the active extrusion of xenobiotics from cells. P-gp is characterized by a high promiscuity toward substrates and is overexpressed in many cancer types.

The work in this manuscript was generously supported by Worldwide Cancer Research (Grant 12-0008).
https://doi.org/10.1124/dmd.118.083188.
[S]This article has supplemental material available at dmd.aspetjournals.org.

**ABBREVIATIONS:** ABC, ATP binding cassette; BBB, blood-brain barrier; CI, combination index; DMSO, dimethylsulfoxide; MTT, 3-(4,5-dimethylthiazol-2-Yl)-2,5-diphenyltetrazolium bromide; NBD, nucleotide binding domain; P-gp, P-glycoprotein; rfu, relative fluorescence unit.

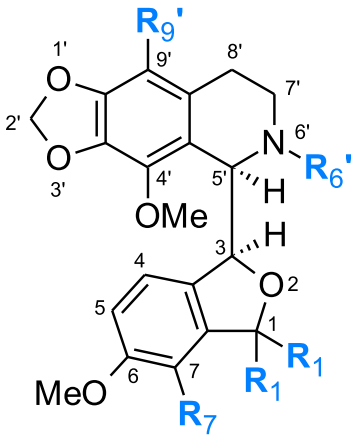


| Compounds | R1 | R7 | R6' | R9' |
|---|---|---|---|---|
| **Noscapine (1)** | =O | OMe | Me | H |
| **2** | =O | OMe | **C(O)OtBu** | H |
| **3** | =O | OMe | **C(O)NHEt** | H |
| **4** | =O | OMe | **C(O)NHEt** | **Cl** |
| **5** | =O | **OH** | **C(O)NHEt** | **Cl** |
| **6** | **H,H** | OMe | **C(O)OPh** | H |
| **7** | **H,H** | OMe | **C(O)NHEt** | H |
| **8** | **H,H** | OMe | **C(O)NHEt** | **Cl** |
| **9** | **H,H** | OMe | **C(O)NHEt** | **Br** |
| **10** | **H,H** | OMe | **C(O)NHEt** | **I** |
| **11** | **H,H** | OMe | **C(O)NHEt** | **$NH_2$** |

**Fig. 1.** Chemical structures of noscapine derivatives. A series of derivatives were generated using noscapine as a template. Chemical substituents were generated at the positions marked $R^1$, $R^{6'}$, $R^7$, and $R^{9'}$. The calculated permeability (cLogP) values were determined using the "molinspiration" property engine v2016.10.

Overexpression in cancer cells confers a resistant phenotype, which is a negative prognostic indicator for chemotherapy (Modok et al., 2006). The prevalence of P-gp– mediated resistance and the breadth of drugs involved have engendered considerable research efforts into developing inhibitors of the pump. An astonishing number of potent inhibitors have been developed; however, none has reached clinical use to date. Consequently, the spectre of P-gp–mediated resistance remains a major consideration for drug development in oncology. Moreover, the protein is expressed in healthy tissues, particularly those involved in secretory roles or in the formation of barriers for sanctuary sites. In fact, the Food and Drug Adminitration and the International Transporter Consortium have published guidelines on the methods and importance of establishing possible interactions of new molecular entities with P-gp (Agarwal et al., 2013).

Despite considerable efforts, the pharmacophore of interaction with P-gp remains unknown, although substrates and inhibitors typically contain a planar hydrophobic ring system and a cationic nitrogen group. It is not possible to predict accurately whether a compound is likely to interact with P-gp. Therefore, the susceptibility of noscapine and its derivatives to P-gp–mediated efflux from cancer cells is unknown. The aim of this investigation was to ascertain whether the potency of a series of multifunctionalized noscapine derivatives to inhibit proliferation is altered in drug-resistant cancer cells. Modified drug potency may indicate an interaction with P-gp since this protein confers a resistant phenotype in these cells. Consequently, the interaction between noscapine derivatives and P-gp was investigated using a series of direct functional assays. Finally, the impact of P-gp expression on synergy between noscapine derivatives and the tubulin disruptor vinblastine was described.

## Materials and Methods

**Cell Culture.** The drug-sensitive human breast adenocarcinoma cell line MCF7 (ATCC HTB-22) was purchased from the American Type Culture Collection (Rockville, MD). The doxorubicin-selected P-gp–expressing variant NCI/$Adr^{Res}$ cell line was obtained from Dr. K. Cowan (National Cancer Institute, Bethesda, MD) and has been verified as a derivative of the $MCF7^{WT}$ line (Mehta et al., 2002). All cell lines were grown at 37°C with 5% $CO_2$ as monolayer cultures in Dulbecco's modified Eagle's medium supplemented with 10% fetal calf serum, penicillin (10,000 U/ml), and streptomycin (10,000 mg/ml). Every third passage of NCI/$Adr^{Res}$ was supplemented with doxorubicin (3 $\mu$M) to maintain selection pressure for resistance. All cells were grown to a maximum of 20 passages of subculture. DNA fingerprint analysis has verified that both cell lines originated from breast cancer tissue and that the NCI/$Adr^{RES}$ cells are derived from the MCF7 line. The NCI/$Adr^{RES}$ cells did, however, contain a minor contaminant of A2780 ovarian cancer cells. Despite the supplementation of medium with doxorubicin, there was no detectable expression of the multidrug transporters ABCG2 or ABCC1 in the NCI/$ADR^{Res}$ cell line as previously reported (Rivers et al., 2008).

**Compound Synthesis.** The compounds used in the study were synthesized as described in DeBono et al. (2012).

**Cell Growth Assay.** Cell growth assays were done as previously described (Muthiah and Callaghan, 2017). Noscapine derivatives, anticancer drugs, and P-gp inhibitors were added from a 2× stock solution in medium (100 $\mu$l) to produce a final concentration range of $10^{-12}$ to $10^{-4}$ M. The solvent (dimethylsulfoxide, DMSO) concentration in the wells was kept to 0.2% (v/v). Cell viability after drug treatment was assessed using the 3-(4,5-dimethylthiazol-2-Yl)-2,5-diphenyltetrazolium bromide (MTT) assay (Mosmann, 1983) after 6 days, at which point the control wells (i.e., DMSO-treated) had reached confluence. The absorbance in the control wells was assigned a value of 100%, and the potency ($IC_{50}$) of each compound to inhibit growth was derived. The absence of selection agent (namely, doxorubicin) during the 6-day period did not alter the expression of P-gp in the NCI/$Adr^{RES}$ cells (Supplemental Fig. 1).

For combination cytotoxicity assays, cells were incubated with vinblastine as described already herein either in the presence or absence of noscapine and its derivatives. Drugs and cells were incubated at 37°C with 5% $CO_2$ for 6 days. The nature of interaction between drugs coadministered in cytotoxicity assays was evaluated using combination indices (CI) that were derived from the Lowe's additivity model (Chou, 2006).

**Calcein-AM Transport in Whole Cells.** The calcein-AM assay to measure the transport function of ABCB1 was based on a modified version (Muthiah and Callaghan, 2017) of a previously published method (Homolya et al., 1993). $MCF7^{WT}$ and NCI/$Adr^{RES}$ cells were seeded into 96-well tissue culture plates at a density of $2 \times 10^3$ cells per well in 100 $\mu$l and allowed to adhere for 2 days at 37°C with 5% $CO_2$. Test compounds (100 $\mu$l) were added from a 2× final concentration in Hanks' balanced salt solution from an original stock solution of 50 mM in DMSO. Calcein-AM was added to a concentration of 1 $\mu$M, and fluorescence was measured at 37°C using an excitation of $\lambda$ = 488 nm and an emission of $\lambda$ = 515 nm.

**Purification and Reconstitution of P-gp.** P-gp was expressed in *Trichoplusia ni* (High-Five; Life Technologies, Mulgrave Vic) cells after infection with recombinant baculovirus as previously described (Taylor et al., 2001). Crude membranes were prepared from the cells using differential ultracentrifugation after cell disruption by nitrogen cavitation. P-gp was purified using immobilized metal affinity chromatography according to previously published methods with some modifications (Taylor et al., 2001; Crowley et al., 2009). The primary difference was

the solubilization of membranes in 2% (w/v) dodecyl-β-D-maltoside supplemented with a 0.4% (w/v) lipid mixture with a 4:1 ratio of *Escherichia coli* extract-to-cholesterol. Reconstitution was achieved by detergent adsorption to SM-2 BioBeads (BioRad, Gladesville NSW) as described (Crowley et al., 2009).

**ATP Hydrolysis Activity of P-gp.** The ATPase activity of P-gp was measured in proteoliposomes based on the rate of inorganic phosphate liberation using a modified colorimetric assay (Chifflet et al., 1988; Crowley et al., 2009). In all cases, the activity was expressed as micromoles of $P_i$ liberated per minute per milligram of pure protein. To determine the Michaelis-Menten parameters, proteoliposomes (0.1–0.5 μg of protein per point) were incubated with ATP (0–1.75 mM) either in the presence of 10 μM nicardipine (i.e., stimulated activity) or with the solvent DMSO (i.e., basal activity). To investigate the potency of drugs to stimulate ATP hydrolysis, activity was measured as a function of added drug concentration ($10^{-9}$–$10^{-4}$ M) in the presence of 2 mM ATP.

**Data Analysis.** Curve-fitting was done using nonlinear or linear least-squares regression, and an *F*-test was used for comparison of multiple curves. The Student's *t* test was used for statistical analyses of two groups and for comparison of three or more groups, a one-way analysis of variance using the Dunnett's post hoc test. *P* values <0.05 were considered statistically significant. All curve-fitting and statistical analyses of data were carried out using GraphPad Prism Software v6 (GraphPad Software, San Diego, CA).

## Results

**Growth Inhibition of Sensitive and Resistant Cancer Cell Lines by Noscapine Derivatives.** Vinblastine produces growth arrest in cells by disrupting microtubules, and this is the basis for its anticancer activity. In the MCF7 breast cancer cell line, the potency of vinblastine to produce growth arrest was $IC_{50}$ = 0.31 ± 0.05 nM, as shown in Fig. 2A. In the NCI/$Adr^{RES}$ cells, the potency of vinblastine to reduce growth was significantly lower ($P < 0.01$) and characterized by an $IC_{50}$ = 159 ± 15 nM. This 512-fold reduction in potency is indicative of the resistant phenotype produced by overexpression of P-gp and the associated efflux of vinblastine from cells. Identical analysis was undertaken for noscapine and the 10 chemically modified derivatives shown in Fig. 1. Modifications were made to four positions of noscapine, namely, the 1, 7, 6′, and 9′positions, as such modification have previously been shown to have a major influence on cytotoxic activity. More specifically, we studied compounds in which the lactone present in the isobenzofuranone ring system was reduced to corresponding cyclic ether (compounds **6**–**11**), the *N*-methyl in the 6′ position was converted to a carbamate (**2** and **6**) or urea moiety (**3**–**5**, **7**–**11**), the 7-methoxy was demethylated to give the corresponding phenol (**5**), and a halogen or amino group was installed in the 9′ position (**4**, **5**, **8**–**11**). The calculated partition coefficient (cLogP) values are provided for noscapine and its derivatives in Fig. 1. Except for compound (**11**), all derivatives displayed higher partition coefficients (cLogP 3.39–4.53) than the parent noscapine (cLogP 2.81).

The growth inhibitory effects of noscapine and two of the derivatives **7** and **3** on MCF7 and NCI/$Adr^{RES}$ cells are shown in Fig. 2, B–D. Noscapine produced growth inhibition in both cell lines, although the potency did not differ between the MCF7 ($IC_{50}$ = 45.4 ± 6.5 μM) and NCI/$Adr^{RES}$ cells ($IC_{50}$ = 32.1 ± 7.0 μM) (Table 1). In addition, the potency of noscapine was considerably lower than the cytotoxic anticancer drug vinblastine. Compound **7** was modified at the 1′ and 6′ positions of the noscapine core (Fig. 1), and this produced a modest increase ($P < 0.01$) in potency for the derivative (Fig. 2C). Like noscapine, however, the growth inhibition produced by **7** was similar in the control and P-gp–expressing cell lines.

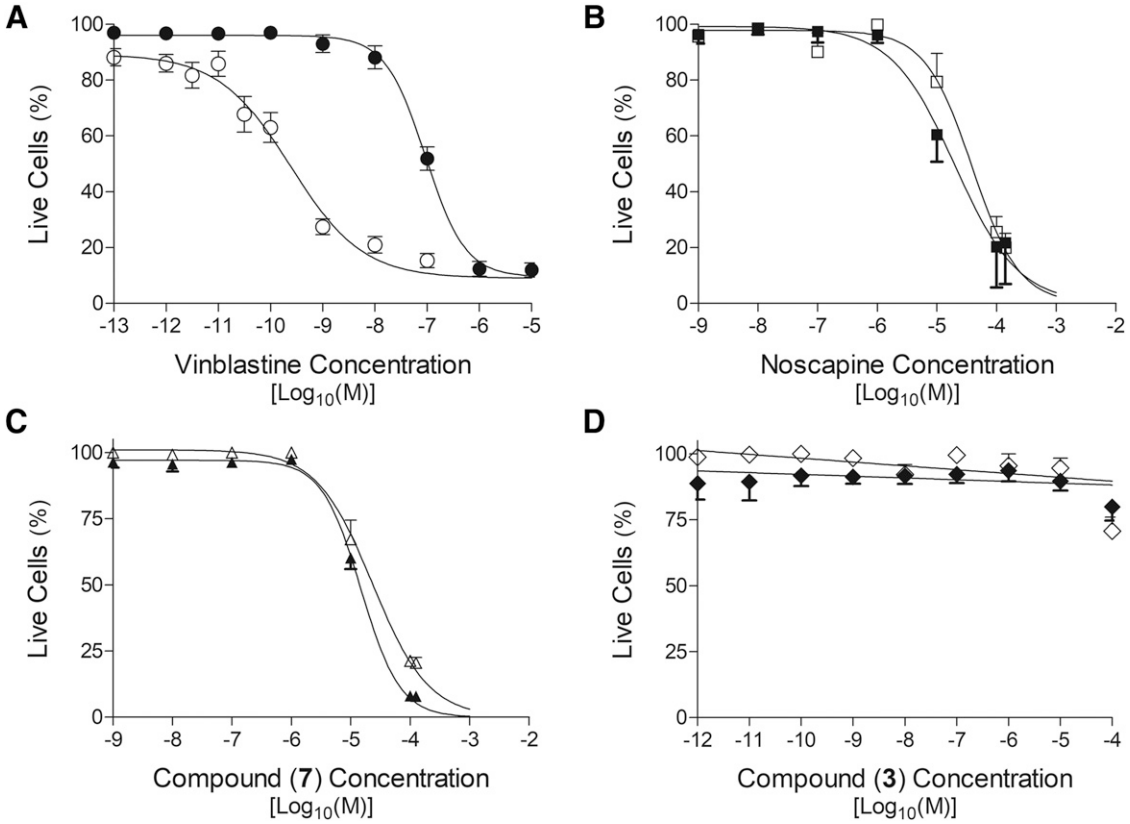


**Fig. 2.** Effects of vinblastine, noscapine, and its derivatives on cell proliferation. Drug- sensitive MCF7 (empty symbols) and the drug-resistant NCI/$Adr^{RES}$ cells (filled symbols) were incubated with drugs for a 6 days as described in the *Materials and Methods*. The percentage of live cells remaining after exposure to (A) vinblastine, (B) noscapine, (C) compound (**7**), or (D) compound (**3**) were determined using the MTT assay. Sigmoidal dose-response curves were fitted using nonlinear regression, and the values correspond to mean ± S.E.M. obtained from at least three independent observations.

TABLE 1

Potency of noscapine and several chemical derivatives to elicit cytotoxicity in drug-sensitive and -resistant breast cancer cell lines

The potencies of drugs to inhibit cell proliferation ($IC_{50}$) were determined using the MTT assay described in the *Materials and Methods*. Values (mean ± S.E.M.) were obtained by nonlinear regression of the general dose-response relationship. The values in parentheses correspond to the number of independent observations.

| Compound | Cytotoxic Potency $IC_{50}$ ($\mu M$) | |
|---|---|---|
| | MCF7 | $NCI/Adr^{RES}$ |
| Noscapine | 45.4 ± 6.5 (13) | 32.1 ± 7.0 (12) |
| (2) | NE (5) | NE (4) |
| (3) | N.E (6) | NE (4) |
| (4) | 5.3 ± 0.9* (6) | 3.3 ± 0.41* (5) |
| (5) | 1.6 ± 0.4* (11) | 6.4 ± 2.4* (4) |
| (6) | 2.5 ± 0.4* (11) | 3.0 ± 0.6* (6) |
| (7) | 14.6 ± 2.5* (8) | 12.6 ± 2.8* (7) |
| (8) | 2.5 ± 0.5* (11) | 2.1 ± 0.5* (6) |
| (9) | 2.3 ± 0.7* (15) | 2.1 ± 0.5* (7) |
| (10) | 4.3 ± 0.7* (7) | 2.4 ± 0.2* (7) |
| (11) | 21.5 ± 7.3* (6) | 18.3 ± 2.8 (3) |

MCF, human breast adenocarcinoma cell line; MTT, 3-(4,5-dimethylthiazol-2-Yl)-2,5-diphenyltetrazolium bromide; NE, compound did not generate a cytotoxic response.

*Statistically significant difference ($P < 0.01$) compared with the value obtained for noscapine in the specific cell line.

The derivative **3** was not able to produce growth inhibition of either cell line at concentrations up to 100 $\mu$M (Fig. 2D). Compound **3** retained the carbonyl group at the $R^1$ position of noscapine but contained a 6′-ethylaminocarbonyl substituent as per compound **7** (Fig. 1). Similarly, compound **2** failed to elicit any growth inhibition at concentrations up to 100 $\mu$M in either cell line (Table 1) and contained a carbonyl substitution at position $R^1$. This substitution did not preclude growth inhibition, as evidenced by the potent activity of **4** and **5** (Table 1). These two derivatives differed from the inactive compounds **2** and **3** at the 7-position ($-OCH_3$ vs. $-OH$) and by the presence of a halide at position $R^{9'}$.

Table 1 provides the potency of four additional noscapine derivatives, and all of them display significantly higher ($P < 0.01$) potency than the parent compound. Another consistent feature was the lack of any difference in potency between the sensitive and resistant cell lines, which suggests that the expression of P-gp does not affect the growth inhibition produced by this series of noscapine derivatives. This is desirable given the ability of this transporter to confound conventional chemotherapy and suggests that the compounds are not substrates for transport by P-gp.

**Effects of Noscapine Derivatives on the Transport Activity of P-gp in Whole Cells.** P-gp is known to interact with more than 300 distinct compounds, but only a proportion of these are substrates for efflux, and numerous compounds directly inhibit its transport activity. Therefore, we investigated the ability of noscapine derivatives to inhibit the transport of a known P-gp substrate, calcein-AM.

Once calcein-AM enters cells, it is rapidly cleaved by esterases to yield the highly fluorescent compound calcein. Calcein appearance, detected as an increase in fluorescence, is shown for representative examples of both cell lines in Fig. 3A. In MCF7 cells, the rate of calcein appearance was 102 ± 2 relative fluorescence units (rfu/min), whereas the rate in $NCI/Adr^{RES}$ cells was markedly lower at 0.17 ± 0.26 rfu/min. The reduced rate of appearance in $NCI/Adr^{RES}$ cells reflects the resistant phenotype attributed to overexpression of P-gp. Addition of the P-gp inhibitor nicardipine caused a dose-dependent increase in the rate of fluorescence in $NCI/Adr^{RES}$ cells (Fig. 3B). In contrast, nicardipine did not alter the rate of calcein accumulation in the drug-sensitive MCF7 cells (data not shown). The accumulation rate of calcein in $NCI/Adr^{RES}$ cells

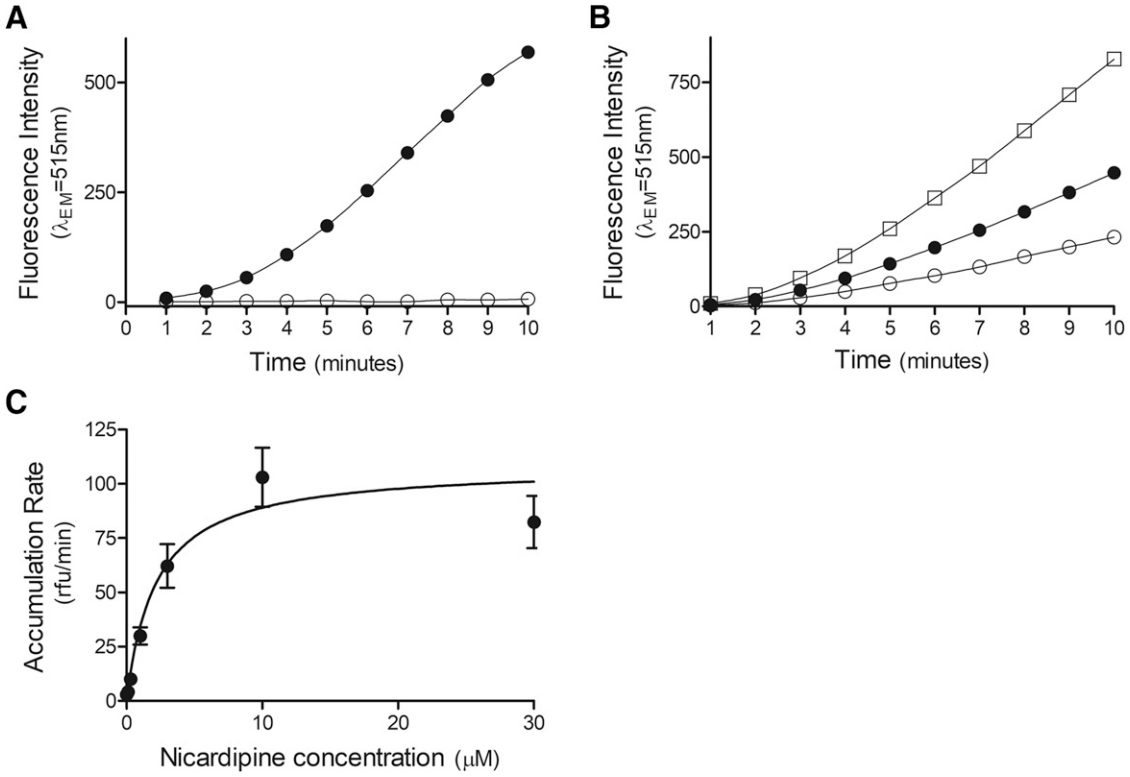


**Fig. 3.** Accumulation of calcein-AM in MCF7 and $NCI/Adr^{RES}$ cells. The transport of calcein-AM (1 $\mu$M) was measured using a fluorescence-based assay in 96-well microplates over a 10-minute period. Liberation of the fluorescent calcein in cells was detected using an excitation $\lambda$ = 488 nm and an emission $\lambda$ = 515 nm. (A) A representative fluorescence-intensity profile measured in MCF7 (●) and $NCI/Adr^{RES}$ (○) cells. (B) The fluorescence intensity was measured in $NCI/Adr^{RES}$ cells in the presence of 1 (○), 3 (●) or 10 $\mu$M (□) nicardipine. The rate of calcein accumulation was determined from the slope between 5 and 10 minutes. (C) The rate of calcein accumulation was plotted as a function of nicardipine, and the data were fitted with a hyperbolic relationship using nonlinear regression. Values correspond to mean ± S.E.M. obtained from at least three independent observations

TABLE 2

Effects of nicardipine and several noscapine derivatives on calcein-AM accumulation in drug-sensitive and -resistant breast cancer cell lines

Accumulation of calcein in NCI/Adr$^{RES}$ cells was determined from the rate of fluorescence change and plotted as a function of added drug concentration. A secondary plot was used to determine the potency of drugs ($MP_{50}$) to alter the accumulation of calcein and the maximal rate ($A_{MAX}$) for this accumulation. Parameters (mean ± S.E.M.) were obtained by nonlinear regression of a hyperbolic equation.

| Compound | *(n)* | Potency $MP_{50}$ | Extent $A_{MAX}$ |
|---|---|---|---|
| | | *μM* | *rfu* |
| Nicardipine | (11) | 2.5 ± 0.6 | 110 ± 19 |
| Noscapine | (9) | 8.5 ± 2.1 | 24.6 ± 6.7 |
| **(2)** | — | nd | nd |
| **(3)** | — | nd | nd |
| **(4)** | (4) | 10.1 ± 2.7 | 145 ± 33* |
| **(5)** | (4) | NE | NE |
| **(6)** | (6) | 0.37 ± 0.07* | 35.1 ± 4.0 |
| **(7)** | (4) | NE | NE |
| **(8)** | (5) | 1.2 ± 0.2* | 137 ± 30* |
| **(9)** | (8) | 6.9 ± 2.0 | 67.6 ± 26.0 |
| **(10)** | (7) | 3.8 ± 1.0 | 76.3 ± 28.7 |
| **(11)** | (4) | 20.9 ± 5.3** | 83.5 ± 21.7 |

(*n*), Number of independent observations. NE, the compound did not alter calcein-AM accumulation; and n.d., no values were determined; rfu, relative fluorescence units.
*Statistically significant difference ($P < 0.05$) compared with the value for noscapine.
**$P < 0.01$.

was plotted as a function of nicardipine concentration to generate the secondary plot (displayed as Fig. 3C). Two parameters were derived from the hyperbolic plot: the potency of nicardipine to increase the rate of calcein accumulation ($MP_{50}$) and the maximal rate of calcein accumulation in the presence of modulator ($A_{MAX}$). In the presence of nicardipine, the rate of calcein accumulation increased to a maximum value of $A_{MAX}$ = 110 ± 19 r.f.u/min, and the potency of nicardipine to increase the rate was $MP_{50}$ = 2.5 ± 0.6 μM (Fig. 3A; Table 2). The $A_{MAX}$ value derived for nicardipine was similar to the rate of calcein appearance in MCF7 cells and suggests complete inhibition of P-gp activity. Noscapine was also capable of increasing the rate of calcein accumulation specifically in NCI/Adr$^{RES}$ cells, although the maximal rate observed was significantly lower at $A_{MAX}$ = 24.6 ± 6.7 rfu/min ($P < 0.05$) (Table 2).

The chemical derivatives of noscapine were also investigated for their ability to modulate the rate of calcein accumulation in NCI/Adr$^{RES}$ cells; the $MP_{50}$ and $A_{MAX}$ values listed in Table 2. Neither **4** nor **7** was able to modulate the rate of calcein appearance in NCI/Adr$^{RES}$ cells at concentrations up to 30 μM. Compound **6** increased the rate of calcein appearance and the value of $A_{MAX}$ = 35.1 ± 4.0 r.f.u/min was not significantly different from noscapine; however, the potency of this derivative to inhibit P-gp activity was significantly greater (Table 2). Compound **4** displayed potency that was indistinguishable from noscapine, whereas it produced the greatest increase in the $A_{MAX}$ parameter of calcein appearance.

Compounds **9**, **10**, and **11** produced a marked increase in the rate of calcein appearance, and **8** generated a significant increase ($P < 0.05$) in $A_{MAX}$ compared with noscapine (Table 2). Compounds **9** and **10** displayed similar potencies to noscapine and contained halide substitutions at the $R^{9'}$ position (Fig. 1). Compound **8** also contained a halide at position $R^{9'}$, but its potency was significantly greater ($P < 0.05$) than that of noscapine. In contrast, **11** produced a similar extent of increase in $A_{MAX}$; however, its potency was the lowest. This compound contained an amino substituent at the 9′ position rather than a halide but identical moieties at the 1′, 7′, and 6' positions.

Overall, most noscapine derivatives were capable of modulating the transport activity of P-gp. Compound **8** was optimal compound from this series for inhibition of P-gp since it markedly increased the rate of calcein appearance and did so with high potency.

**Do Noscapine Derivatives Interact Directly with Purified, Reconstituted P-gp?** The noscapine derivatives may affect the cellular transport activity of P-gp by acting as specific inhibitors or through an indirect mechanism. To discriminate between these possibilities, P-gp was purified and reconstituted into liposomes to enable direct investigation of the interaction of noscapine derivatives with the protein. P-gp uses the energy of ATP hydrolysis to drive vectorial transport, and both substrates and inhibitors have been demonstrated to dramatically stimulate the rate of catalysis.

The ATPase activity of P-gp was measured as a function of varying concentrations of ATP in the absence or presence of nicardipine (Fig. 4). In the absence of nicardipine, the basal rate of ATP hydrolysis was characterized by a maximal activity of $V_{MAX}$ = 213 ± 19 nmol $P_i$/min per milligram and an affinity constant for ATP of $K_M$ = 1.31 ± 0.14 mM. In the presence of nicardipine the rate of ATP hydrolysis was significantly ($P < 0.01$) increased ($V_{MAX}$ = 904 ± 66 nmol $P_i$/min per milligram), but with no significant change in the affinity constant ($K_M$ = 0.71 ± 0.06 mM). The data demonstrate that both the maximal

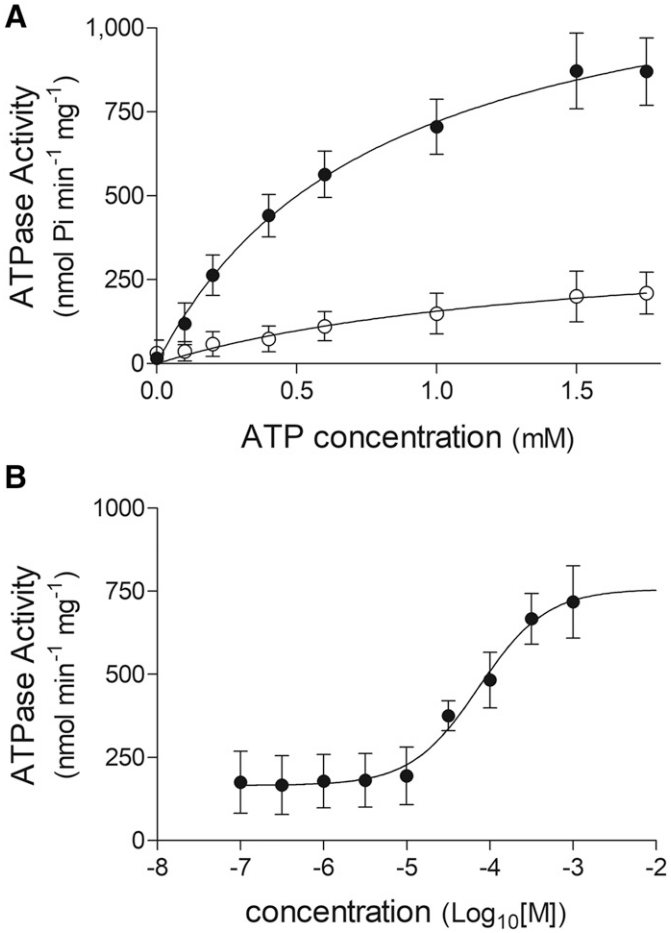


**Fig. 4.** Drug stimulation of ATP hydrolysis by purified P-gp. The ATPase activity of P-gp was measured by the appearance phosphate using a colorimetric assay. Proteoliposomes (0.1–0.5 μg protein) were incubated with ATP and drug as indicated to follow. (A) ATP hydrolysis by purified P-gp was measured with a range of ATP concentrations (0–1.75 mM) in the absence (○) or presence (●) of nicardipine (10 μM) for 30 minutes. The Michaelis-Menten equation was fitted to the data using nonlinear regression. (B) The ATPase activity of P-gp was measured in the presence of ATP (2 mM) and a series of noscapine concentrations ($10^{-7}$–$10^{-3}$M) for 30 minutes. A sigmoidal dose-response curve was fitted to the data using nonlinear regression. The rate of ATP hydrolysis was normalized for both protein content and the assay time, and values represent mean ± S.E.M. obtained from five independent observations.

rate of ATP hydrolysis and the degree of stimulation by nicardipine were similar to values published by our laboratories (Taylor et al., 2001; Mittra et al., 2017). Moreover, this confirms the integrity of the purified P-gp preparations and enables their use to characterize interaction with noscapine and its derivatives.

We used a modified ATPase assay to enable characterization of drug interaction with purified P-gp. In particular, the rate of hydrolysis was measured in the presence of a range of drug concentrations to ascertain the potency of interaction with P-gp. Figure 4B shows the effect of noscapine on the rate of ATP hydrolysis. The ATPase activity was stimulated by noscapine from 163 ± 71 nmol $P_i$/min per milligram to a value of 744 ± 149 nmol $P_i$/min per milligram. The 3.4 ± 0.4-fold stimulation of ATPase activity was described by a sigmoidal relationship with a potency of 44.6 ± 9.1 $\mu$M for noscapine. Identical analysis was undertaken for each of the noscapine derivatives and for nicardipine (Table 3).

Although the degree of stimulation by noscapine was not different from that of nicardipine, its potency was significantly lower ($P < 0.01$). As detailed in Table 3, most noscapine derivatives were able to stimulate ATP hydrolysis by purified P-gp, and the extent of this stimulation (1.4- to 4.4-fold) did not differ significantly from the parent compound noscapine or the P-gp modulator nicardipine. Only **10** and **11** were unable to affect the ATPase activity at the concentrations tested; however, the range of potencies was large; **3** ($EC_{50}$ = 65.3 ± 10.2 $\mu$M) was the least potent and **4** ($EC_{50}$ = 0.95 ± 0.28 $\mu$M) the most potent.

The results demonstrate that the noscapine derivatives can interact directly with purified P-gp, and this direct interaction with P-gp is responsible for the inhibition of calcein-AM transport. In addition, the equipotent growth inhibitory effects of the noscapine derivatives between the resistant and sensitive cell lines suggest that the compounds are not substrates for transport and thereby act as specific inhibitors of P-gp. As such, it is conceivable that the noscapine derivatives may potentiate the effects of cytotoxic drugs, particularly in P-gp–expressing resistant cells.

**Do Noscapine Derivatives Improve the Anticancer Activity of Vinblastine?** Noscapine was coadministered with the anticancer drug vinblastine to ascertain the potential for potentiated inhibition of cellular proliferation. The cytotoxicity profile of vinblastine in the absence or presence of noscapine is shown in Fig. 5 for both drug-resistant and -sensitive cells. The addition of noscapine caused a reduction in the upper limit of the dose-response curve for vinblastine in MCF7 cells (Fig. 5A). This reduction is presumably due to the growth inhibitory effects of noscapine per se (Fig. 2B). In contrast, the potency of vinblastine was not significantly altered. For example, in MCF7 cells, the potency of vinblastine alone was $IC_{50}$ = 0.059 ± 0.029 nM, and in the presence of the highest concentration of noscapine (30 $\mu$M), it was unchanged at $IC_{50}$ = 0.063 ± 0.014 nM.

TABLE 3

Effects of nicardipine and several noscapine derivatives on the rate of ATP hydrolysis by purified, reconstituted P-glycoprotein (P-gp)

The ATPase activity of purified P-gp was measured using a colorimetric assay and plotted as a function of added drug concentration. The general dose-response relationship was fitted to the data to determine the potency to stimulate hydrolysis ($EC_{50}$) and the extent of stimulation. Values correspond to mean ± S.E.M.

| Compound | (*n*) | Potency | Stimulation |
|---|---|---|---|
| | | *$EC_{50}$ ($\mu$M)* | *Fold basal* |
| Nicardipine | (6) | 2.9 ± 0.5** | 5.3 ± 0.5 |
| Noscapine | (6) | 44.6 ± 9.1 | 3.4 ± 0.4 |
| **(2)** | (3) | 4.1 ± 1.6** | 2.5 ± 0.3 |
| **(3)** | (2) | 65.3 ± 10.2 | 4.4 ± 1.3 |
| **(4)** | (3) | 0.95 ± 0.28** | 2.4 ± 0.4 |
| **(5)** | (6) | 18.7 ± 4.5** | 3.1 ± 0.3 |
| **(6)** | (4) | 1.0 ± 0.4** | 1.4 ± 0.9 |
| **(7)** | (6) | 19.1 ± 1.4** | 2.7 ± 0.7 |
| **(8)** | (4) | 10.1 ± 5.3** | 2.2 ± 0.3 |
| **(9)** | (3) | 22.5 ± 5.8* | 2.8 ± 0.6 |
| **(10)** | (4) | NE | NE |
| **(11)** | (3) | NE | NE |

(*n*), Number of independent observations; NE, compound did not alter ATP hydrolysis by G-gp.
*Statistically significant difference compared with noscapine ($P < 0.05$).
**$P < 0.01$.

The dose-response profiles in P-gp–expressing NCI/$Adr^{RES}$ cells displayed a reduction in the upper limit and a shift to higher potency (Fig. 5B). The cytotoxic potency of vinblastine alone was $IC_{50}$ = 188 ± 65 nM, and the addition of 10 $\mu$M noscapine caused no significant change to the potency ($IC_{50}$ = 157 ± 41 nM); however, the addition of 20 $\mu$M noscapine increased the apparent vinblastine potency 9.6-fold to $IC_{50}$ = 19 ± 7 nM. The reduction of the upper limit of the dose-response curves was broadly similar to that observed in MCF7 cells.

Isobologram analysis was undertaken to determine whether the alteration in the efficacy and potency of vinblastine produced by noscapine was additive or synergistic. The drug-drug interactions were analyzed by determination of combination indices (CI) at each concentration of noscapine. The reduction in the upper limit of the dose-response relationships necessitated the use of an $IC_{75}$ value since the coaddition of >10 $\mu$M noscapine resulted in cell viability falling below 50%. The CI values (Table 4) were plotted for the combination of vinblastine and noscapine in both cell lines (Fig. 5, C and D).

In the MCF7 cells, the CI values obtained for at each noscapine concentration differed significantly from 1.0 (Table 4) and were located in the sector below the line of additivity in the isobologram (Fig. 5C), thus indicating a synergistic interaction. Similarly, in NCI/$Adr^{RES}$ cells, the CI values for the two highest concentrations of noscapine were also significantly different from 1.0 (Table 4) and were also located below the isobole in Fig. 5D. Therefore, the synergistic relationship between noscapine and vinblastine was retained in the P-gp–expressing NCI/$Adr^{RES}$ cells.

The CI analysis was also undertaken for two derivatives of noscapine, namely, **6** and **8** (Table 4). These two derivatives were chosen based on their high potency and efficacy to cause growth inhibition of the cell lines and to modulate the transport activity of P-gp. In the case of **6**, only the highest concentration tested (3 $\mu$M) demonstrated synergy with vinblastine in the MCF7 cells; however, there was a greater propensity of **6** to generate a synergistic effect with vinblastine in NCI/$Adr^{RES}$ cells.

Compound **8** produced a dramatic reduction in the upper limit of dose-response relationships, and CI could not be determined for concentrations above 0.3 $\mu$M in the MCF7 cells and above 1 $\mu$M in NCI/$Adr^{RES}$ cells (Table 4). There was no synergy between **8** and vinblastine in the MCF7 cells, albeit with a narrow range of concentrations. In contrast, a 1 $\mu$M concentration of compound **8** was able to produce a synergistic effect on cell proliferation with vinblastine in the drug-resistant NCI/$Adr^{RES}$ cell line.

In summary, noscapine and the two derivatives examined were able to inhibit cell proliferation in a synergistic manner with vinblastine. Moreover, there was a higher predisposition for a synergistic interaction in the P-gp–expressing, drug-resistant cells.

## Discussion

Noscapine and several derivatives can modulate the efflux of drugs by P-gp in resistant cancer cells. The modulation is by a direct interaction of the compounds with P-gp, given their ability to alter the activity of purified protein. However, the expression of P-gp in cells did not alter

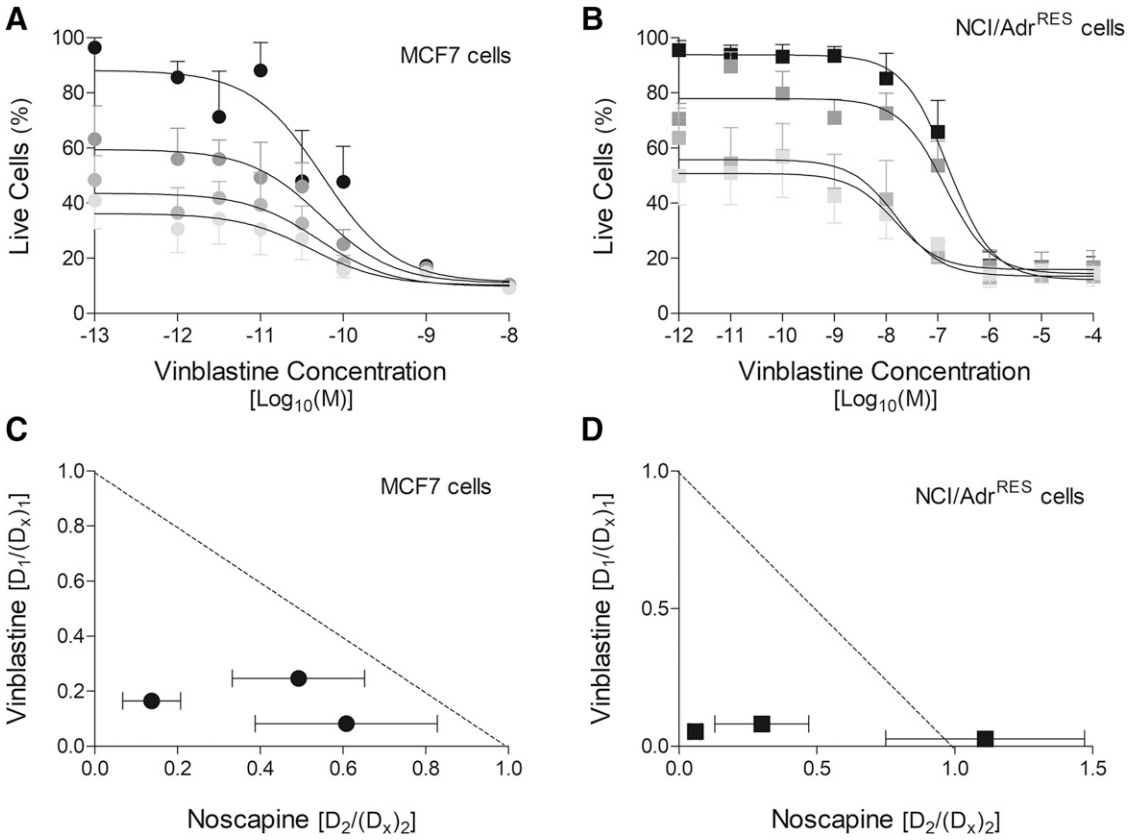


**Fig. 5.** Effects of vinblastine and noscapine coadministration on cell proliferation. Cell proliferation was measured in MCF7 and NCI/Adr$^{RES}$ cells in the presence of vinblastine and a series of noscapine concentrations. Cell viability was measured using the MTT assay after a 6-day incubation with drugs. (A) The effects of vinblastine on the growth of MCF7 cells in the absence (●) or presence of 10 (●), 20 (●), or 30 $\mu$M (●) noscapine. A sigmoidal dose-response relationship was fitted to the data by nonlinear regression. (B) The effects of vinblastine on the growth of NCI/Adr$^{RES}$ cells in the absence (■■■) or presence of 10 (■■■), 20 (■■■), or 30 $\mu$M (■■■) noscapine. A sigmoidal dose-response relationship was fitted to the data by nonlinear regression. (C) Isobologram for the interaction between vinblastine and noscapine in NCI/Adr$^{RES}$ cells. Dose ratios are plotted for data obtained using 10, 20, and 30 $\mu$M noscapine, and the dotted line represents the isobole. (D) Isobologram for the interaction between vinblastine and noscapine in MCF7 cells. Dose ratios are plotted for data obtained using 10, 20, and 30 $\mu$M noscapine, and the dotted line represents the isobole

the potency of noscapine and its derivatives to inhibit proliferation. This finding suggests that the compounds are not substrates for transport by P-gp and act as inhibitors of the protein. These properties of noscapine derivatives enabled synergy with vinblastine to inhibit the proliferation of P-gp–expressing resistant cancer cells. The inherent antiproliferative activity and the ability to "evade" P-gp render the noscapine derivatives potentially innovative tools in chemotherapy regimens.

Substrates for transport by P-gp show reduced accumulation in cells expressing the protein, and in the case of anticancer drugs, this resulted in impaired inhibition of proliferation (Bellamy et al., 1988; Mazzanti et al., 1992; Martin et al., 1999). Inhibition of P-gp–mediated transport should increase the intracellular accumulation of anticancer drugs and restore chemotherapy efficacy. This strategy has been used to identify an arsenal of P-gp inhibitors, beginning with verapamil, through to the most potent compounds tariquidar (XR9576) and elacridar (GF120918) (Tsuruo et al., 1981; Hyafil et al., 1993; Martin et al., 1999).

Unlike transported substrates of P-gp, noscapine derivatives were equipotent between the resistant and sensitive cell lines. The simplest explanation is that noscapine derivatives do not interact with P-gp. However, the derivatives inhibited the calcein-AM transport by P-gp in whole cells. Moreover, the compounds altered the ATPase activity of purified P-gp, which demonstrates that they modulate function by a direct interaction. Should the noscapine derivatives therefore be classified as nontransported inhibitors of P-gp?

The transport mechanism of P-gp requires multiple conformational transitions and the involvement of two distinct domains (Callaghan et al., 2006; Callaghan et al., 2012). Specifically, substrate translocation involves transition of the binding site from a high-affinity and *inward-facing* to a low-affinity and *outward-facing* configuration (Martin et al., 2001; Rosenberg et al., 2001; Al-Shawi et al., 2003; Omote et al., 2004). Efficient transmembrane translocation requires a sufficiently large differential between the binding affinities of a substrate for the two configurations. Moreover, the conformational transitions are intimately linked (i.e., *coupled*) to the discrete stages of the ATP hydrolytic process in the nucleotide binding domains (NBDs).

In general, substrates for transport tend to stimulate the ATPase activity of P-gp and display tight coupling between binding sites and NBDs (Muller et al., 1996; Orlowski et al., 1996). Inhibitors, or modulators, have been demonstrated to bind to P-gp and either stimulate (nicardipine) or inhibit (tariquidar) the overall rate of ATP hydrolysis (Martin et al., 1999; Mittra et al., 2017). Whole-cell transport assays have demonstrated that [$^3$H]-tariquidar is a nontransported substrate for P-gp. Transepithelial transport and permeability assays indicated that nicardipine is also unlikely to be a substrate for transport by P-gp (Lentz et al., 2000). It is therefore difficult to ascertain whether a compound is a substrate or a "classic" inhibitor of P-gp by its effects on ATPase activity. In fact, whether the ATPase activity of P-gp is stimulated or inhibited by a compound is dependent on the kinetics of 1) conformational transitions or 2) dissociation from the outward facing configuration (Martin et al., 2001; Al-Shawi et al., 2003).

TABLE 4

Combination index (CI) analysis of the cytotoxicity of noscapine derivatives coadministered with vinblastine with in drug-sensitive and -resistant breast cancer cell lines

CI values were determined for the effects of coadministration of vinblastine and noscapine derivatives on cell proliferation. Complete dose-response relationships were determined for vinblastine in the absence or presence of the indicated concentrations of noscapine, (**6**) and (**8**). All values (mean ± S.E.M.) were obtained from three independent observations.

| Compound | Conc | Combination Index | |
|---|---|---|---|
| | | MCF7 | NCI/Adr$^{RES}$ |
| | $\mu$M | | |
| Noscapine | 10 | 0.69 ± 0.02** | 1.13 ± 0.362 |
| | 20 | 0.26 ± 0.05** | 0.11 ± 0.02* |
| | 30 | 0.33 ± 0.08** | 0.19 ± 0.06* |
| (**6**) | 0.1 | 1.64 ± 0.33 | 1.10 ± 0.35 |
| | 0.3 | 1.04 ± 0.46 | 0.49 ± 0.25 |
| | 1 | 1.11 ± 0.35 | 0.33 ± 0.15* |
| | 3 | 0.59 ± 0.02** | 0.24 ± 0.04** |
| (**8**) | 0.1 | 2.57 ± 1.01 | 2.11 ± 0.89 |
| | 0.3 | 0.62 ± 0.36 | 0.75 ± 0.22 |
| | 1 | *n*.d. | 0.52 ± 0.27* |
| | 3 | n.d. | n.d. |

Conc., concentration; MCF, human breast adenocarcinoma cell line; n.d., no values were determined.

*$P < 0.05$; **$P < 0.01$ indicate a statistically significant difference from the isobole, which is defined with CI = 1.

The effects of noscapine derivatives on the proliferation of resistant cells and the activity of P-gp support their classification as nontransported inhibitors. Further evidence has been provided by the pharmacokinetics of noscapine in vivo (Landen et al., 2004). The oral administration of noscapine in mice produced growth inhibition of glioblastoma and did so after rapid passage across the blood-brain barrier (BBB). It is well established that P-gp is expressed and active in endothelial cells of the BBB, where it regulates the entry, or exit, of compounds to the central nervous system (Jette et al., 1993; Agarwal et al., 2011; Auvity et al., 2018). Substrates for P-gp are prevented from entering the central nervous system, and the ability of noscapine to cross the BBB indicates that it is not subject to efflux by P-gp.

It may also be possible for the noscapine derivatives to "bypass" the actions of P-gp if their permeability is sufficiently high, resulting in rapid and extensive intracellular accumulation. Diffusional permeability of cells to drugs is in part dictated by their partition coefficients into the membrane; however, the cLogP values are broadly similar to those of vinblastine and paclitaxel, both substrates of the transporter. This observation does not to support a model whereby noscapine and derivatives bypass P-gp through kinetic factors. The compounds potentially act in a similar manner to that described for tariquidar, namely, as a nontransported P-gp modulator (Martin et al., 1999).

Synergism between anticancer drugs has long been viewed as a promising strategy to improve inhibition of tumor growth (Merlin, 1994). Noscapine and vinblastine bind to distinct sites on tubulin and synergy of activity is a distinct possibility. The present investigation has demonstrated synergism between noscapine and two derivatives with vinblastine. Another vinca alkaloid (vinorelbine) also displays synergy with paclitaxel, another tubulin-disrupting drug that interacts at a distinct site (Photiou et al., 1997). In addition, noscapine also synergizes with paclitaxel (Altinoz et al., 2006) and two tubulin binding compounds with anticancer activity in vitro, peloruside and laulimalide (Gajewski et al., 2012). Similarly, a noscapine derivative, 9′-bromonoscapine, in combination with docetaxol, produced a apoptotic response, mitotic arrest, and inhibition of tumor growth in a synergistic manner (Pannu et al., 2011). However, synergistic behavior of noscapine and its derivatives is not limited to tubulin-disrupting compounds. For example, noscapine was also demonstrated to potentiate the activity of cisplatin (DNA cross-linking) and the alkylating agents temozolamide and bis-chloroethylnitrosurea (BCNU) in glioblastoma cells and in xenograft models (Qi et al., 2013). Therefore, the noscapine derivatives provide the potential to reduce the dose of conventional genotoxic anticancer drugs and maintain significant tumor growth inhibition. Moreover, the inherently low toxicity of noscapine and a reduced dose of genotoxic drugs may diminish the limiting side effects of chemotherapy. The synergy with approved anticancer drugs will require extensive pharmacokinetic investigation to fully validate this potential of noscapine in chemotherapy.

Drug interactions with tubulin have been extensively characterized for numerous antiproliferative agents. For example, it has been demonstrated, using structural modeling, that colchicine and noscapine bind to the same, or an overlapping, site on tubulin (Naik et al., 2011). In contrast, vinblastine and colchicine are known to interact at distinct sites on tubulin (Luduena and Roach, 1981; Wolff et al., 1991). By inference, noscapine and vinblastine alter tubulin dynamics through interaction at distinct sites, which may result in synergistic effects on cell proliferation. The synergistic interaction between noscapine derivatives and vinblastine raises the issue of where the two compounds interact on P-gp. Despite the availability of several structures for P-gp (Aller et al., 2009; Alam et al., 2018; Kim and Chen, 2018), the location of drug-binding sites remains elusive, although biochemical approaches are beginning to shed detailed information (Loo et al., 2009; Mittra et al., 2017). Thus, it is not yet possible to assign the respective sites for vinblastine and noscapine binding on P-gp, but the differing interactions with tubulin support distinct sites.

As discussed earlier, the search for compounds to inhibit P-gp activity and restore accumulation of anticancer drugs has been exhaustive; however, the search has not yielded any clinically used inhibitors, primarily because of pharmacokinetic issues. Consequently, the need for novel strategies to overcome the actions of P-gp has been touted (Callaghan et al., 2014). The ability of noscapine to evade P-gp–mediated efflux and to potentiate the activity of vinblastine in drug-resistant cells provides a major benefit. A similar property is shared with the epothilones, which also alter microtubule dynamics and inhibit mitosis in cancer cells, including an equipotent effect in P-gp–expressing cells (Alberti, 2013). Furthermore, a 9′-nitro-noscapine derivative has been shown to elicit apoptosis and mitotic arrest in ovarian and T-cell lymphoma cell lines known to express P-gp and displaying resistance to paclitaxel and vinblastine (Aneja et al., 2006a).

The noscapine derivatives appear to short-circuit the resistant phenotype conferred by P-gp; namely, they can avoid efflux from cells by the pump and yet can inhibit its activity. Moreover, the ability to potentiate the efficacy of conventional anticancer drugs presents a unique strategy to restore chemotherapy in drug-resistant cancer. Noscapine has long been established to display low toxicity and is well tolerated in its therapeutic setting as an antitussive agent (Mahmoudian and Rahimi-Moghaddam, 2009). Furthermore, pharmacokinetic studies in healthy volunteers indicate that low micromolar plasma concentrations may be attained via both oral and intravenous administration of noscapine (Dahlstrom et al., 1982). Moreover, noscapine displayed the lowest potency of the derivatives tested in this study. and the latter also displayed improved partition coefficients. The improved potencies and high partition coefficients of the noscapine derivatives raise the possibility of them reaching plasma levels sufficient to facilitate restoration of chemotherapeutic success and diminish the actions of P-gp.

**Authorship Contributions**

*Participated in tesearch design*: Callaghan, Scammells, Muthiah.

*Conducted experiments:* Muthiah, Henshaw, DeBono.

*Contributed new reagents or analytic tools:* DeBono, Capuano, Scammells.
*Performed data analysis:* Muhiah, Henshaw, Callaghan.
*Wrote or contributed to the writing of the manuscript:* Callaghan, Muthiah, Capuano, Scammells.

## References


Agarwal S, Arya V, and Zhang L (2013) Review of P-gp inhibition data in recently approved new drug applications: utility of the proposed [I(1) ]/IC(50) and [I(2) ]/IC(50) criteria in the P-gp decision tree. *J Clin Pharmacol* **53**:228–233.

Agarwal S, Hartz AM, Elmquist WF, and Bauer B (2011) Breast cancer resistance protein and P-glycoprotein in brain cancer: two gatekeepers team up. *Curr Pharm Des* **17**:2793–2802.

Alam A, Küng R, Kowal J, McLeod RA, Tremp N, Broude EV, Roninson IB, Stahlberg H, and Locher KP (2018) Structure of a zosuquidar and UIC2-bound human-mouse chimeric ABCB1. *Proc Natl Acad Sci USA* **115**:E1973–E1982.

Alberti C (2013) Taxane- and epothilone-based chemotherapy: from molecule cargo cytoskeletal logistics to management of castration-resistant prostate carcinoma. *Eur Rev Med Pharmacol Sci* **17**:1658–1664.

Aller SG, Yu J, Ward A, Weng Y, Chittaboina S, Zhuo R, Harrell PM, Trinh YT, Zhang Q, Urbatsch IL, et al. (2009) Structure of P-glycoprotein reveals a molecular basis for poly-specific drug binding. *Science* **323**:1718–1722.

Al-Shawi MK, Polar MK, Omote H, and Figler RA (2003) Transition state analysis of the coupling of drug transport to ATP hydrolysis by P-glycoprotein. *J Biol Chem* **278**:52629–52640.

Altinoz MA, Bilir A, Del Maestro RF, Tuna S, Ozcan E, and Gedikoglu G (2006) Noscapine and diltiazem augment taxol and radiation-induced S-phase arrest and clonogenic death of C6 glioma in vitro. *Surg Neurol* **65**:478–485.

Anderson JT, Ting AE, Boozer S, Brunden KR, Crumrine C, Danzig J, Dent T, Faga L, Harrington JJ, Hodnick WF, et al. (2005a) Identification of novel and improved antimitotic agents derived from noscapine. *J Med Chem* **48**:7096–7098.

Anderson JT, Ting AE, Boozer S, Brunden KR, Danzig J, Dent T, Harrington JJ, Murphy SM, Perry R, Raber A, et al. (2005b) Discovery of S-phase arresting agents derived from noscapine. *J Med Chem* **48**:2756–2758.

Aneja R, Vangapandu SN, Lopus M, Chandra R, Panda D, and Joshi HC (2006a) Development of a novel nitro-derivative of noscapine for the potential treatment of drug-resistant ovarian cancer and T-cell lymphoma. *Mol Pharmacol* **69**:1801–1809.

Aneja R, Vangapandu SN, Lopus M, Viswesarappa VG, Dhiman N, Verma A, Chandra R, Panda D, and Joshi HC (2006b) Synthesis of microtubule-interfering halogenated noscapine analogs that perturb mitosis in cancer cells followed by cell death. *Biochem Pharmacol* **72**:415–426.

Auvity S, Caille F, Marie S, Wimberley C, Bauer M, Langer O, Buvat I, Goutal S, and Tournier N (2018) P-glycoprotein (ABCB1) inhibits the influx and increases the efflux of $^{11}$C-metoclopramide across the blood-brain barrier: a PET study on nonhuman primates. *J Nucl Med* **59**:1609–1615

Bellamy WT, Dalton WS, Kailey JM, Gleason MC, McCloskey TM, Dorr RT, and Alberts DS (1988) Verapamil reversal of doxorubicin resistance in multidrug-resistant human myeloma cells and association with drug accumulation and DNA damage. *Cancer Res* **48**:6365–6370.

Callaghan R, Ford RC, and Kerr ID (2006) The translocation mechanism of P-glycoprotein. *FEBS Lett* **580**:1056–1063.

Callaghan R, George AM, and Kerr ID (2012) 8.8 molecular aspects of the translocation process by ABC proteins, in *Comprehensive Biophysics* (Edward HE ed) pp 145–173, Elsevier, Amsterdam.

Callaghan R, Luk F, and Bebawy M (2014) Inhibition of the multidrug resistance P-glycoprotein: time for a change of strategy? *Drug Metab Dispos* **42**:623–631.

Chifflet S, Torriglia A, Chiesa R, and Tolosa S (1988) A method for the determination of inorganic phosphate in the presence of labile organic phosphate and high concentrations of protein: application to lens ATPases. *Anal Biochem* **168**:1–4.

Chou TC (2006) Theoretical basis, experimental design, and computerized simulation of synergism and antagonism in drug combination studies. *Pharmacol Rev* **58**:621–681.

Crowley E, O'Mara ML, Reynolds C, Tieleman DP, Storm J, Kerr ID, and Callaghan R (2009) Transmembrane helix 12 modulates progression of the ATP catalytic cycle in ABCB1. *Biochemistry* **48**:6249–6258.

Dahlström B, Mellstrand T, Löfdahl CG, and Johansson M (1982) Pharmacokinetic properties of noscapine. *Eur J Clin Pharmacol* **22**:535–539.

Debono AJ, Mistry SJ, Xie J, Muthiah D, Phillips J, Ventura S, Callaghan R, Pouton CW, Capuano B, and Scammells PJ (2014) The synthesis and biological evaluation of multifunctionalised derivatives of noscapine as cytotoxic agents. *ChemMedChem* **9**:399–410.

DeBono AJ, Xie JH, Ventura S, Pouton CW, Capuano B, and Scammells PJ (2012) Synthesis and biological evaluation of N-substituted noscapine analogues. *ChemMedChem* **7**:2122–2133.

Dumontet C, Duran GE, Steger KA, Beketic-Oreskovic L, and Sikic BI (1996) Resistance mechanisms in human sarcoma mutants derived by single-step exposure to paclitaxel (Taxol). *Cancer Res* **56**:1091–1097.

Empey DW, Laitinen LA, Young GA, Bye CE, and Hughes DT (1979) Comparison of the antitussive effects of codeine phosphate 20 mg, dextromethorphan 30 mg and noscapine 30 mg using citric acid-induced cough in normal subjects. *Eur J Clin Pharmacol* **16**:393–397.

Gajewski MM, Alisaraie L, and Tuszynski JA (2012) Peloruside, laulimalide, and noscapine interactions with beta-tubulin. *Pharm Res* **29**:2985–2993.

Homolya L, Holló Z, Germann UA, Pastan I, Gottesman MM, and Sarkadi B (1993) Fluorescent cellular indicators are extruded by the multidrug resistance protein. *J Biol Chem* **268**: 21493–21496.

Hyafil F, Vergely C, Du Vignaud P, and Grand-Perret T (1993) In vitro and in vivo reversal of multidrug resistance by GF120918, an acridonecarboxamide derivative. *Cancer Res* **53**: 4595–4602.

Jetté L, Têtu B, and Béliveau R (1993) High levels of P-glycoprotein detected in isolated brain capillaries. *Biochim Biophys Acta* **1150**:147–154.

Kim Y and Chen J (2018) Molecular structure of human P-glycoprotein in the ATP-bound, outward-facing conformation. *Science* **359**:915–919.

Landen JW, Hau V, Wang M, Davis T, Ciliax B, Wainer BH, Van Meir EG, Glass JD, Joshi HC, and Archer DR (2004) Noscapine crosses the blood-brain barrier and inhibits glioblastoma growth. *Clin Cancer Res* **10**:5187–5201.

Lentz KA, Polli JW, Wring SA, Humphreys JE, and Polli JE (2000) Influence of passive permeability on apparent P-glycoprotein kinetics. *Pharm Res* **17**:1456–1460.

Loo TW, Bartlett MC, and Clarke DM (2009) Identification of residues in the drug translocation pathway of the human multidrug resistance P-glycoprotein by arginine mutagenesis. *J Biol Chem* **284**:24074–24087.

Ludueña RF and Roach MC (1981) Interaction of tubulin with drugs and alkylating agents. 2: effects of colchicine, podophyllotoxin, and vinblastine on the alkylation of tubulin. *Biochemistry* **20**:4444–4450.

Mahmoudian M and Rahimi-Moghaddam P (2009) The anti-cancer activity of noscapine: a review. *Recent Patents Anticancer Drug Discov* **4**:92–97.

Martin C, Berridge G, Mistry P, Higgins C, Charlton P, and Callaghan R (1999) The molecular interaction of the high affinity reversal agent XR9576 with P-glycoprotein. *Br J Pharmacol* **128**: 403–411.

Martin C, Higgins CF, and Callaghan R (2001) The vinblastine binding site adopts high- and low-affinity conformations during a transport cycle of P-glycoprotein. *Biochemistry* **40**:15733–15742.

Mazzanti R, Croop JM, Gatmaitan Z, Budding M, Steiglitz K, Arceci R, and Arias IM (1992) Benzquinamide inhibits P-glycoprotein mediated drug efflux and potentiates anticancer agent cytotoxicity in multidrug resistant cells. *Oncol Res* **4**:359–365.

Mehta K, Devarajan E, Chen J, Multani A, and Pathak S (2002) Multidrug-resistant MCF-7 cells: an identity crisis? *J Natl Cancer Inst* **94**:1652–1654, author reply 1654.

Merlin JL (1994) Concepts of synergism and antagonism. *Anticancer Res* **14** (6A):2315–2319.

Mishra RC, Karna P, Gundala SR, Pannu V, Stanton RA, Gupta KK, Robinson MH, Lopus M, Wilson L, Henary M, et al. (2011) Second generation benzofuranone ring substituted noscapine analogs: synthesis and biological evaluation. *Biochem Pharmacol* **82**:110–121.

Mittra R, Pavy M, Subramanian N, George AM, O'Mara ML, Kerr ID, and Callaghan R (2017) Location of contact residues in pharmacologically distinct drug binding sites on P-glycoprotein. *Biochem Pharmacol* **123**:19–28.

Modok S, Mellor HR, and Callaghan R (2006) Modulation of multidrug resistance efflux pump activity to overcome chemoresistance in cancer. *Curr Opin Pharmacol* **6**:350–354.

Mosmann T (1983) Rapid colorimetric assay for cellular growth and survival: application to proliferation and cytotoxicity assays. *J Immunol Methods* **65**:55–63.

Müller M, Bakos E, Welker E, Váradi A, Germann UA, Gottesman MM, Morse BS, Roninson IB, and Sarkadi B (1996) Altered drug-stimulated ATPase activity in mutants of the human multidrug resistance protein. *J Biol Chem* **271**:1877–1883.

Muthiah D and Callaghan R (2017) Dual effects of the PI3K inhibitor ZSTK474 on multidrug efflux pumps in resistant cancer cells. *Eur J Pharmacol* **815**:127–137.

Naik PK, Santoshi S, Rai A, and Joshi HC (2011) Molecular modelling and competition binding study of Br-noscapine and colchicine provide insight into noscapinoid-tubulin binding site. *J Mol Graph Model* **29**:947–955.

Omote H, Figler RA, Polar MK, and Al-Shawi MK (2004) Improved energy coupling of human P-glycoprotein by the glycine 185 to valine mutation. *Biochemistry* **43**:3917–3928.

Orlowski S, Mir LM, Belehradek J, Jr, and Garrigos M (1996) Effects of steroids and verapamil on P-glycoprotein ATPase activity: progesterone, desoxycorticosterone, corticosterone and verapamil are mutually non-exclusive modulators. *Biochem J* **317**:515–522.

Pannu V, Karna P, Sajja HK, Shukla D, and Aneja R (2011) Synergistic antimicrotubule therapy for prostate cancer. *Biochem Pharmacol* **81**:478–487.

Photiou A, Shah P, Leong LK, Moss J, and Retsas S (1997) In vitro synergy of paclitaxel (Taxol) and vinorelbine (navelbine) against human melanoma cell lines. *Eur J Cancer* **33**:463–470.

Qi Q, Liu X, Li S, Joshi HC, and Ye K (2013) Synergistic suppression of noscapine and conventional chemotherapeutics on human glioblastoma cell growth. *Acta Pharmacol Sin* **34**: 930–938.

Rivers F, O'Brien TJ, and Callaghan R (2008) Exploring the possible interaction between antiepilepsy drugs and multidrug efflux pumps; in vitro observations. *Eur J Pharmacol* **598**:1–8.

Rosenberg MF, Velarde G, Ford RC, Martin C, Berridge G, Kerr ID, Callaghan R, Schmidlin A, Wooding C, Linton KJ, et al. (2001) Repacking of the transmembrane domains of P-glycoprotein during the transport ATPase cycle. *EMBO J* **20**:5615–5625.

Taylor AM, Storm J, Soceneantu L, Linton KJ, Gabriel M, Martin C, Woodhouse J, Blott E, Higgins CF, and Callaghan R (2001) Detailed characterization of cysteine-less P-glycoprotein reveals subtle pharmacological differences in function from wild-type protein. *Br J Pharmacol* **134**:1609–1618.

Tsuruo T, Iida H, Tsukagoshi S, and Sakurai Y (1981) Overcoming of vincristine resistance in P388 leukemia in vivo and in vitro through enhanced cytotoxicity of vincristine and vinblastine by verapamil. *Cancer Res* **41**:1967–1972.

Wolff J, Knipling L, Cahnmann HJ, and Palumbo G (1991) Direct photoaffinity labeling of tubulin with colchicine. *Proc Natl Acad Sci USA* **88**:2820–2824.

Ye K, Ke Y, Keshava N, Shanks J, Kapp JA, Tekmal RR, Petros J, and Joshi HC (1998) Opium alkaloid noscapine is an antitumor agent that arrests metaphase and induces apoptosis in dividing cells. *Proc Natl Acad Sci USA* **95**:1601–1606.


**Address correspondence to:** Richard Callaghan, Research School of Biology, Building 134, Linnaeus Way, Australian National University, Acton, Canberra, ACT 2601, Australia. E-mail: richard.callaghan@anu.edu.au